

Segmentation of Optic Disc in Fundus Images using Convolutional Neural Networks for Detection of Glaucoma

R. Priyanka¹, Prof. S. J. Grace Shoba², Dr. A. Brintha Therese³

¹M.E Applied Electronics, Velammal Engineering College Chennai, India

²Professor Velammal Engineering College, Chennai, India

³Professor /SENSE, VIT University, Chennai, India

Abstract— The condition of the vascular network of human eye is an important diagnostic factor in ophthalmology. Its segmentation in fundus imaging is a difficult task due to various anatomical structures like blood vessel, optic cup, optic disc, macula and fovea. Blood vessel segmentation can assist in the detection of pathological changes which are possible indicators for arteriosclerosis, retinopathy, microaneurysms and macular degeneration. The segmentation of optic disc and optic cup from retinal images is used to calculate an important indicator, cup-to-disc ratio (CDR) accurately to help the professionals in the detection of Glaucoma in fundus images. In this proposed work, an automated segmentation of anatomical structures in fundus images such as blood vessel and optic disc is done using Convolutional Neural Networks (CNN). A Convolutional Neural Network is a composite of multiple elementary processing units, each featuring several weighted inputs and one output, performing convolution of input signals with weights and transforming the outcome with some form of nonlinearity. The units are arranged in rectangular layers (grids), and their locations in a layer correspond to pixels in an input image. The spatial arrangement of units is the primary characteristics that makes CNNs suitable for processing visual information; the other features are local connectivity, parameter sharing and pooling of hidden units. The advantage of CNN is that it can be trained repeatedly so more features can be found. An average accuracy of 95.64% is determined in the classification of blood vessel or not. Optic cup is also segmented from the optic disc by Fuzzy C Means Clustering (FCM). This proposed algorithm is tested on a sample of hospital images and CDR value is determined. The obtained values of CDR is compared with the given values of the sample images and hence the performance of proposed system in which Convolutional Neural Networks

for segmentation is employed, is excellent in automated detection of healthy and Glaucoma images.

Keywords— Fundus images ,blood vessel segmentation ,global contrast normalization ,zero phase component analysis, convolutional neural networks, Optic cup and disc, FCM.

I. INTRODUCTION

Glaucoma is a typical eye illness that is irreversible and the second driving reason for visual impairment. Because of absence of a powerful early screening framework it end up noticeably mindful just in the last phases of glaucoma. The quantity of individuals with glaucoma was 64.3 million, and is expected to ascend to 76.0 million in 2020. Early analysis and treatment are essential to avoid loss of vision in glaucoma patients. Glaucoma can be recognized right on time by checking retinal fundus images condition. The fundus image of the eye incorporates the retina, optic circle, fovea, macula and back post. Retinal fundus images have remained the top standard for assessing the adjustments in retina. Out of the few techniques utilized for clinical determination of glaucoma, fundus image examination is the one most appropriate for recognizing. A programmed framework for glaucoma location is proposed here, which makes utilization of fundus image utilizing CDR. The optic disc (OD) or optic nerve head in the retina where cell axons leave the eye to shape the optic nerve. Optic disc division utilizing CNN is the initial phases in the proposed approach. The optic disc has a focal wretchedness, denied of sensory tissue. Glaucoma, described by loss of nerve tissue causes extending of this disc area, happening in the prevalent and substandard localitiess in the early stages. Optic cup is segmented by Fuzzy C means utilizing ROI and morphological operation. The parameter Cup-to-Disc Ratio is figured to check for glaucoma. The retina is the

inward most essential layer of the eye where the fastest obsessive changes can be seen. It is made out of a few vital anatomical structures, for example, optic disc, fovea, macula and veins which can show numerous sicknesses that cause visual loss. The optic disc is the brightest part in the typical fundus image that can be viewed as a pale, round or vertically marginally oval plate. It is the opening of veins and optic nerves to the retina and it regularly fills in as a point of interest and reference for alternate elements in fundus images. Figure 1 represents a fundus images. The optic cup is a two-walled gloom that can be found in the focal point of the eye's optic disc. This zone is named for its area and cup like shape. The optic cup is one of the segments of the visual system. The fovea is the inside most part of the macula. The modest region is in charge of our focal, most keen vision. A solid fovea is key perusing, sitting in front of the driving, and different exercises that require the capacity to see detail. The macula is found generally in the focal point of the retina, transient to the optic nerve. It is exceptionally touchy piece of retina is capable of point by point focal vision. The fovea is the exceptionally focus of the macula. In the focal point of retina is the optic nerve, a round to oval white territory that measures around 2 x 1.5 mm over. From the focal point of the optic nerve transmits the real blood two and half plate distances across to one side of the disc, can be seen the somewhat oval molded. The retina is a layered tissue coating the inside surface of the eye. It changes over approaching light to the activity potential which is further prepared in the visual focuses of the cerebrum. Retina is one of a veins that can be specifically identified non-invasively. It is of incredible reason in prescription to picture the retina and create calculations for investigating those pictures. Late innovation in most recent a quarter century to the improvement of advanced retinal imaging frameworks. The retinal vessels are associated and make a parallel treelike structure, however some foundation elements may likewise have comparable ascribes to vessels.

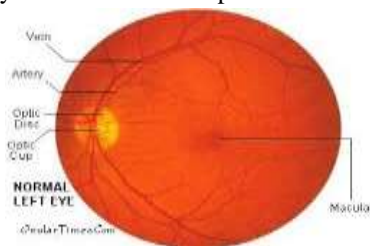


Fig.1: Retinal fundus image

A few morphological components of retinal veins and courses have symptomatic importance so can be utilized as

a part of checking the infection, treatment, and assessment of different cardiovascular and ophthalmologic diseases due to the manual vein division is a tedious and dreary undertaking which requires preparing, programmed division of retinal vessels is the underlying stride in the advancement of a PC helped demonstrative framework for ophthalmic issue . Programmed division of the veins in retinal pictures is vital in recognizing the number of eye infections in light of the fact that now and again they influence vessel tree itself. In different cases (e.g. obsessive injuries) the execution of programmed discovery might be enhanced if vein tree is prohibited from the examination. Thus the programmed vessel division shapes a pivotal segment of any robotized screening framework. Manufactured Neural Systems (NNs) have an amazing record of uses in image examination and understanding, including medicinal imaging.

II. RELATED WORK

Segmentation methods can be divided into unsupervised and supervised. In the former ones, the properties of structures to be detected are manually hard-coded into algorithm's structure, and learning is limited or altogether absent. In the unsupervised methods category, algorithms that apply matched filtering, vessel tracking, morphological transformations and model-based algorithms are predominant. In the matched filtering-based method [1], a 2-D linear structuring element is used to extract a Gaussian intensity profile of the retinal blood vessels, using Gaussian derivatives, for vessel enhancement. The structuring element is rotated 8-12 times to fit the vessels in different configurations to extract the boundary of the vessels. This method has high time complexity since a stopping criterion is evaluated for each end pixel. In another vessel tracking method [2], Gabor filters are designed to detect and extract the blood vessels. This method suffers from over-detection of blood vessel pixels due to the introduction of a large number of false edges. A morphology based method in [3] combines morphological transformations with curvature information and matched-filtering for centerline detection. This method has high time complexity due to the vessel center-line detection followed by vessel filling operation, and it is sensitive to false edges introduced by bright region edges such as optic disc and exudates. Another morphology based method [4] in uses multiple structuring elements to extract vessel ridges followed by connected component analysis. In another model-based method [5], blood vessel structures are extracted by convolving with a Laplacian kernel followed by thresholding and connecting broken line

components. An improvement of this methodology was presented in [6], where the blood vessels are extracted by the Laplacian operator and noisy objects are pruned according to center lines. This method focuses on vessel extraction from images with bright abnormalities, but it does not perform very effectively on retinal images with hemorrhages or microaneurysms. In [10] a new hybrid approach called genetic algorithm for blood vessel detection which uses geometrical parameters. There are two methods proposed in [12] that uses the line detectors to detect the presence of blood vessel in image pixel. In [13] co-occurrence matrix is calculated and thresholding decision is made from the matrix. Automatic segmentation of vessel using B-Cosfire filter by collinear aligned difference of Gaussian [14]. In [15] a new infinite contour model for the detection of blood vessel that uses hybrid information. All such unsupervised methods are either computationally intensive or sensitive to retinal abnormalities. In supervised methods, segmentation algorithms acquire the necessary knowledge by learning from image patches annotated by ground truth. For instance in [9], ridge features (zero-crossings of brightness derivative) are detected, grouped, and fed into a nearest-neighbor classifier. In [16], a multiscale Gabor transform (wavelets) is used to extract features from a patch, and train Bayesian classifiers on them. In [17], a morphology-based method detects the evident vessels and background areas, while a Gaussian mixture model classifies the more difficult pixels. These methods use training data to train a classifier using SVM [18]. to train a classifier However these method are not purely supervised in the strict meaning of this term, as the network learns from features defined by a human expert. According to, the only purely neural and thus fully supervised approach (i.e., with a network directly applied to image patches) was presented in, which however contained only visual inspection of the resulting segmentations and did not report objective quality measures. In the context of the past work, the method proposed in this paper should be classified as supervised: no prior domain knowledge on vessel structure was used for its design. Glaucoma is the common cause of blindness with about 79 million in the world likely to be afflicted with glaucoma by the year 2020 [19].

Glaucoma is asymptotic in the early stages and its early detection and subsequent treatment is essential to prevent visual damage [20]. There have been efforts to automatically detect glaucoma from 3-D images [21], [22]. However, due to their high cost they are generally unavailable at primary care centers Gopal and Jayanthi

proposed an automated OD Parameterization techniques for segmenting optic disc and cup from retinal images [23]. In 2011, another researcher Rajendra et al. proposed a texture feature based technique for identifying Glaucoma retinal images [24]. Another automated system for the detection of Glaucoma from the fundus image as proposed by Chalinee et al. [25]. They extracted disc through edge detection method and level set method then cup was segmented using color component analysis method. Gopal Dat joshi proposed another technique for intensity changes in vessels minimization using active contour in specific region, though deformation of cup will not be constant due to changes in vessels [26]. S Chandrika and K. Nirmala detected Glaucoma by k-mean clustering and Gabor wavelet transform technique from which they have computed CDR [27]. Cup-to-disc ratio (CDR) is the most famous indicator. Cup to disc ratio is calculated by using a optic cup diameter divided by a optic disc diameter [28]. Optic disc margin, neuroretinal rim, cup-to-disc ratio and optic disc hemorrhages are some examples of clinical indicators that use to evaluate glaucoma [29]. Optic disc margin, neuroretinal rim, cup-to-disc ratio and optic disc hemorrhages are some examples of clinical indicators that use to evaluate glaucoma [30].

III. DEEP LEARNING

Many models intended to work with image information, specifically convolutional systems (CNNs), were routinely manufactured as of now in 1970's and figured out how to discover business applications and outperform different methodologies on testing errands like manually written character acknowledgment. In any case, the break of centuries saw recognizable stagnation in spite of exceptional research endeavors, NNs neglected to scale well with errand unpredictability. The beginning of option ML procedures, similar to support vector machines and Bayesian systems, incidentally downgraded the NNs, and it was just the generally late entry of profound learning (DL) that brought them once more into the spotlight. Today, expansive scale DL-prepared NNs effectively handle bland protest acknowledgment undertakings with a huge number of question classes, an accomplishment that many considered unbelievable before ten years. The capacities of profound NNs came from a few improvements. Transfer elements of units in traditional NNs are normally crushing capacities (sigmoid or hyperbolic digression), with subordinates near zero all over the place. This prompts lessening the angle for preparing the backpropagated mistakes rapidly diminish with each system layer, rendering

inadequate or agonizingly moderate. Interestingly, these capacities utilized as a part of profound CNNs, most outstandingly correcting straight units don't vanish in extremes, thus permit powerful preparing of systems with many layers. Also, DL carried with it new strategies for boosting system heartiness like dropout where haphazardly chose units that are incidentally crippled. This powers a system to shape weight setup, that give adjust yields regardless of the possibility that some picture elements are missing, thus enhances speculation.. In this paper, we propose a DL-based technique for the issue of distinguishing blood vessels and optical cup and disc in fundus symbolism, a medicinal imaging undertaking that has huge analytic pertinence and was liable to many reviews in the past. The proposed approach beats past techniques on two noteworthy execution markers, i.e., precision of characterization and territory under the ROC bend. We consider a few system models and image preprocessing strategies, confirm the outcomes on three picture databases, perform cross-check between the databases, analyse the outcomes against the past techniques, and investigate the divisions outwardly.

IV. METHODS AND METHODOLOGY

The first step is to segment the blood vessels in retinal fundus images with convolutional neural networks, involves following steps

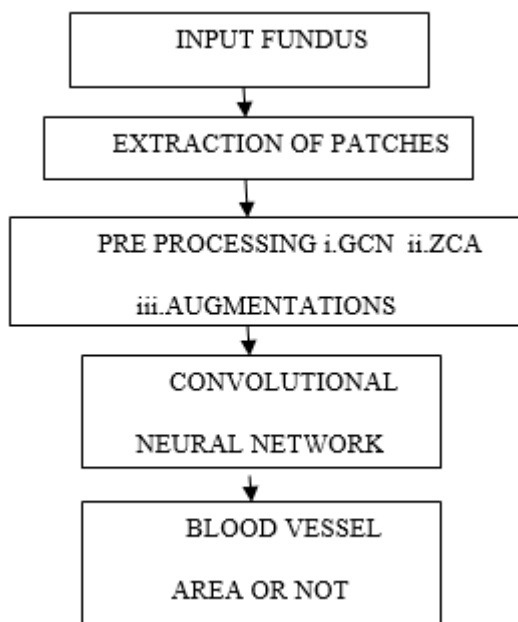


Fig.2: block diagram of the blood vessel segmentation

A) Extraction Of Patches

The ground-truth data provided in the handbook segmentations frames the blood vessel detection as a binary classification problem. As in many other studies, in our approach the decision on the class of a particular pixel is based on an $m \times m$ patch centered at that pixel. A triple of such patches, each reflecting image content at the same location for the RGB channels, forms the input fed into a neural network. Together with the associated class label of the central pixel, it forms an example. In this study, we use $m = 27$, so an example is a vector of length $3 \times 27 \times 27 = 2187$.

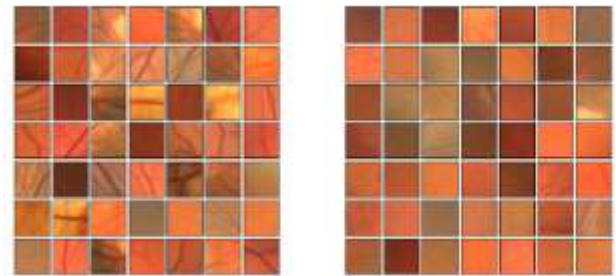


Fig.3: Patches of the input image

B) Global Contrast Normalization

The images clearly specify that brightness may vary across the FOV. In order to help the learning process to abstract from these fluctuations and focus on vessel detection, we perform local (per-patch) brightness and contrast normalization. Every patch is standardized by subtracting the mean and dividing by the standard deviation of its elements (independently in the R, G, and B channel), which also maps the originally byte-encoded brightness to signed reals.

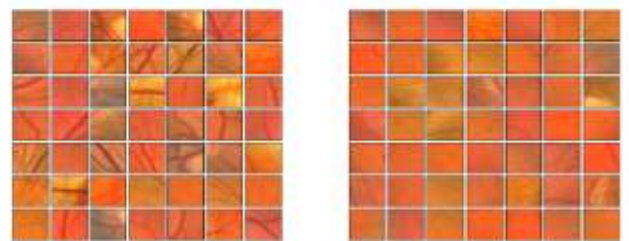


Fig.4: Global contrast normalization

C) Zero-Phase Component Analysis

In natural images, neighboring pixels are strongly connected as they are likely to represent the same structure in a scene. When learning an algebraic model of images (which is what a neural network is essentially doing), it is thus desirable to abstract from these universal

characteristics and focus on the higher-order correlations, i.e., capture the relevant regularities rather than the quite obvious fact that nearby pixels are likely to be similar. Removal of universal correlations can be achieved by multiplying the data matrix by a whitening matrix. After this common in DL transformation, it becomes unfeasible to expect the value of one pixel given the value of only one other pixel.

Formally, let the centered (zero mean) data be stored in matrix X with features in columns and data points in rows. In our case, X has $3 \times 27 \times 27 = 2187$ columns and the number of rows equal to the number of examples (patches). Let the covariance matrix have eigenvectors in columns of U and eigen values on the diagonal, so that $SIGMA = U \cdot U^T$. Then, U is an orthogonal rotation matrix, and U^T gives a rotation needed to decorrelate the data (i.e., it maps the original features onto the principal components). The classical PCA whitening transformation is given by:

$$W = \Lambda^{1/2} \cdot U^T$$

Each component of WPCA has variance given by the related eigenvalue. However, whitening is not unique; the whitened data remains whitened under rotation, which means that any $W = RWPCA$ with an orthogonal matrix R will also be a whitening transformation. In what is called zero-phase component analysis (ZCA) whitening, we take U as this orthogonal matrix, i.e.:

$$W = U \cdot \Lambda^{1/2} \cdot U^T$$

In experiments, we first apply GCN to individual patches in the training set, then learn the ZCA transformation from these patches, and finally apply it to convolutional neural networks.

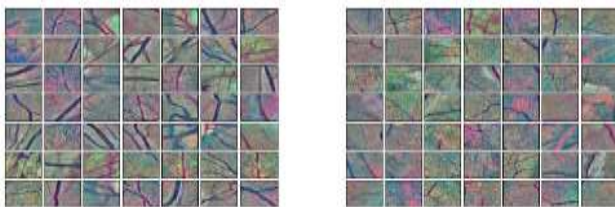


Fig.5: Zero phase component analysis

D) Augmentations

Despite using large numbers of relatively small (27X 27) patches for training, the CNNs may overfit. Other works on deep learning show that the reason for that is the still relatively small number of examples compared to the number of model (CNN's) parameters, which for the network is in the order of 48 millions. The remedy commonly used in deep learning is augmentation, meant as generation of additional examples by (typically

randomized) transformations of existing training examples. The data was enlarged offline, prior to learning. Each patch, normalized and whitened and was subject to 10 independent transformations, each composed of four randomized actions from the following list:

- _ Scaling by a factor between 0.7 and 1.2,
- _ Rotation by an angle from $[-90; 90]$,
- _ Flipping horizontally or vertically,
- _ Gamma correction of Saturation and Value (of the HSV colorspace) by raising pixels to a power in $[0.25; 4]$.

E) Convolutional Neural Networks

A convolutional neural network (CNNs) is a composite of multiple elementary processing units, each featuring several weighted inputs and one output, performing convolution of input signals with weights and transforming the outcome with some form of nonlinearity. The units are arranged in rectangular grids, and their locations in a layer correspond to pixels in an input image. The spatial arrangement of units is the primary characteristics that makes CNNs suitable for processing visual information; the other features are local connectivity, parameter sharing and pooling of hidden units.

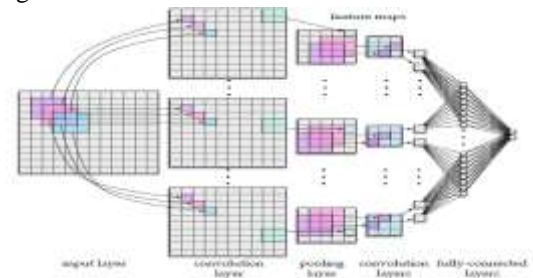


Fig.6: Convolutional neural network

Local connectivity means that a given unit receives data only from its receptive field (RF), a small rectangle of image pixels (for the units in the first layer) or units in the previous layer (for the subsequent layers). The RFs of neighboring units in a layer typically offset by stride. Image size, RF size and stride together determine the dimensions of a layer. For instance, a layer of units with 3×3 RFs with one pixel stride needs only 9 units when applied to a 5×5 monochromatic image, because three RFs of width 3 each, overlapping by two pixels, span the entire image. Larger stride and larger RFs lead to smaller layers. Local connectivity significantly reduces the number of weights in contrast to the fully-connected conventional networks. It is also consistent with the spatial nature of visual information and mimics certain aspects of natural visual systems.

Parameter sharing consists in sharing weights across units in the same layer. When the units in a given layer share the same vector of weights, they form a feature map, with each of them calculating the same local feature, even though from a different part of the image. This reduces the number of parameters even further and makes the extracted features equivariant. For instance, a layer of units with 3×3 RFs connected to a single channel image has only 10 parameters (nine per channel for the pixels in the RF and one for neuron threshold), regardless the number of units.

Pooling consists in aggregating outputs of multiple units by other means than convolution. In the most popular aggregation scheme, max-pooling, each aggregating unit returns the maximum value in its RF. Like local connectivity, pooling reduces the resolution w.r.t. previous layer and provides for translational invariance.

A typical CNN architecture consists of several convolutional feature maps entwined with max-pooling layers, finalized with at least one fully-connected layer that 'funnels' the excitations into output neurons, each corresponding to one decision class. Sliding RFs by the number of pixels defined in stride across the input image causes successive layers to be smaller, so that the final grid fed into the fully connected is usually much smaller than the input image. There are often several feature maps working in parallel, each of them responsible for extracting one feature. Large networks may involve even several dozens of feature maps. In case of multi-channel images, separate feature maps are connected to all channels. The consequent layers fetch data from multiple maps in the previous layer and so combine the information from particular channels. In such a case, each unit has multiple RFs with separate weight vectors, and the weighted signals coming from all input maps together form its excitation.

F) Optic Disc and Cup Segmentation

The next step is to segment cup and disc in fundus images and to calculate the CDR ratio to detect presence of Glaucoma. The block diagram is

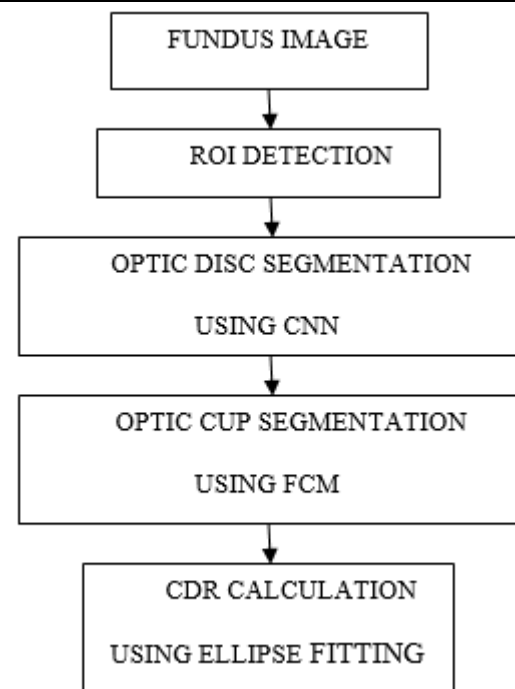


Fig.7: Block diagram of cup and disc segmentation

G) Region Of Interest Detection (ROI)

For the calculation of cup to disc ratio first step is optic cup and optic disc segmentation. Figure 8 is showing framework for the calculation of CDR. In order to detect optic cup or disc, Fundus images are taken by the high resolution retinal fundus camera. Firstly the region of interest which is around optic disc is depicted as shown in the Figure 8. If ROI is detected accurately it will generate small image which will fasten the speed of CDR calculation. Normally its size ranges less than 11% of fundus image. ROI can be found in large number of retinal images without human interruption and it is effective for mass screening. It is found that optic disc area is having higher intensity as compare to the surrounding area of the retinal fundus image. Optic disc center is selected as the point having highest intensity. An approximate high intensity region is calculated via intensity weighted centroid method that would be called as optic disc center. A rectangle twice the diameter of the optic disc is drawn around the ROI known as ROI Boundary which is used for optic disc and cup segmentation.

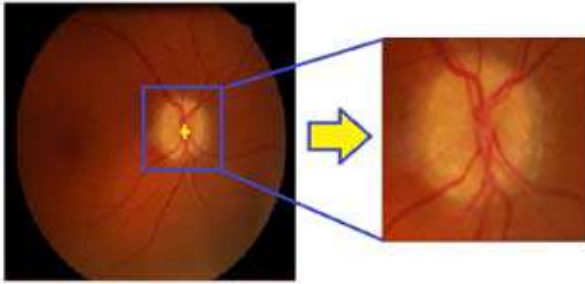


Fig.8: ROI Extration

H) Optic Disc Segmentation

Detection of the OD is a fundamental task for automated diagnosis of various ophthalmic diseases like glaucoma, diabetic retinopathy and pathological myopia. Hence, there is a huge literature available on segmentation of the OD. The OD segmentation estimate the OD boundary using convolutional neural networks in section E.

I) Optic Cup Segmentation

After OD segmentation, the next stage is optic cup segmentation. Optic cup segmentation using Fuzzy C Means.

Fuzzy c-means is a method of clustering which allows one piece of data to belong to two or more clusters. It is based on minimization of the objective function:

$$J_m = \sum_{i=1}^N \sum_{j=1}^C u_{ij}^m \|x_i - c_j\|^2 \quad 1 \leq m < \infty$$

Where $\|*\|$ is any norm expressing similarity between any measured data and the center. m is real number greater than 1, the degree of membership is U_{ij} of x_i in the cluster j , the i th of d -dimensional measured data is x_i , the d -dimension center of the cluster is c_j , Fuzzy partitioning is carried out through an minimization of the objective function shown above, with the update of u_{ij} and the cluster c_j by:

$$u_{ij} = \frac{1}{\sum_{k=1}^C \left(\frac{\|x_i - c_j\|}{\|x_i - c_k\|} \right)^{\frac{2}{m-1}}}, \quad c_j = \frac{\sum_{i=1}^N u_{ij}^m \cdot x_i}{\sum_{i=1}^N u_{ij}^m}$$

$$\max_{ij} \left\{ \left| u_{ij}^{(k+1)} - u_{ij}^{(k)} \right| \right\} < \varepsilon$$

This iteration will stop when $\max_{ij} \left\{ \left| u_{ij}^{(k+1)} - u_{ij}^{(k)} \right| \right\} < \varepsilon$, where ε is a termination criterion between 0 and 1, where k are the number of iteration steps. This procedure converges to a saddle point of J_m .

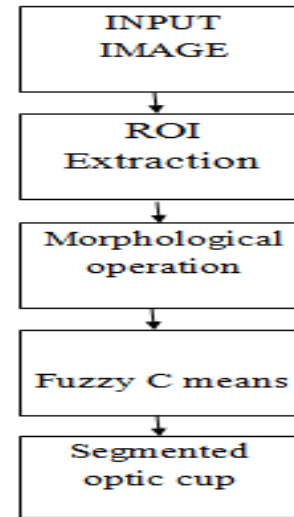


Fig.9: Block diagram for cup segmentation

J) Ellipse Fitting

The ellipse fitting algorithm can be used to smooth the disc and cup boundary. Ellipse fitting is usually based on least square fitting algorithm which assumes that the best-fit curve of a given type is the curve that minimizes the algebraic distance over the set of N data points in the least square. By minimizing the algebraic distance subject to the constraint $4ac^2 + b^2 = 1$, the new method incorporates the ellipticity constraint. It is the best to fit the optic disc and cup since it minimizes the algebraic distance subject to a constraint, and incorporates the elliptic constraint into the normalization factor. It is ellipse-specific, so that effect of noise (ocular blood vessel, hemorrhage, etc.) around the cup area can be minimized while forming the ellipse. It can also be easily solved naturally by a generalized Eigenvalue system. An approximate round estimation of cup boundary is applied as the best fitting least square ellipse. The area enclosed within the ellipse can be considered as the cup and disc surfaces when CDR is calculated by this method

K) Glaucoma Detection

Several parameters used for glaucoma detection such as cup-to disc ratio (CDR), cup-to-disc area ratio, neuro-retinal rim thickness etc. can be found out using this approach.

Cup-to-Disc Ratio: Cup-to-disc ratio is a Significant parameter indicating the expansion of the cup region. Glaucoma tends to affect the superior and inferior regions of the optic nerve first, thereby producing visual field defects. Therefore, CDR, a measure of elongation of the

cup vertically can be used to detect glaucoma in early stages. CDR value of 0.5 and above is a sign of glaucoma

$$\text{CDR} = \frac{\text{DIAMETER OF CUP}}{\text{DIAMETER OF DISC}}$$

V EXPERIMENTAL RESULTS

I) Blood Vessel Segmentation

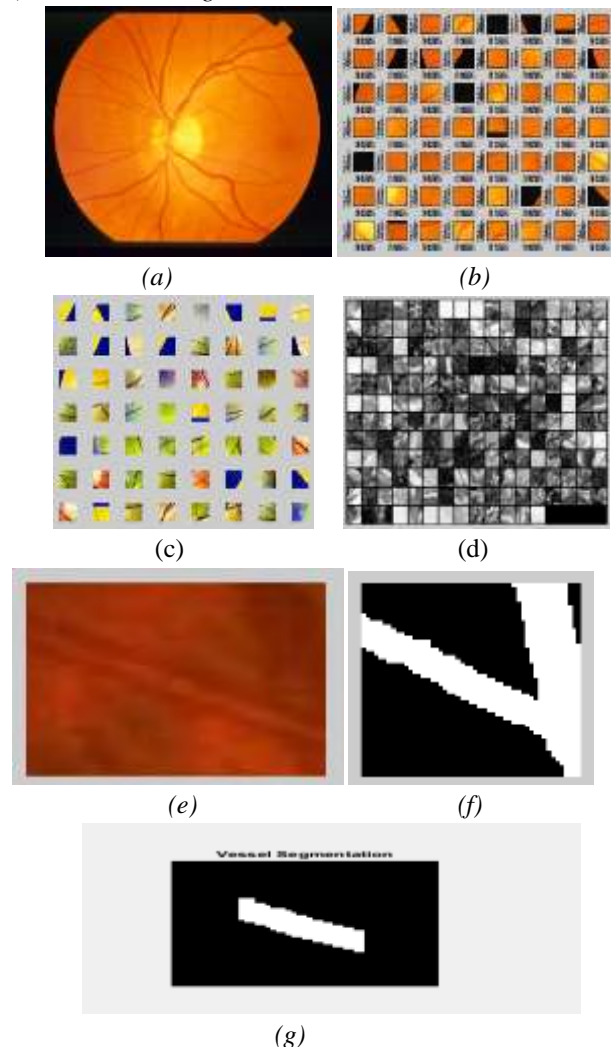


Fig.10: (a) Fundus image (b) Patches of the image (c) GCN (d) ZCA (e) Particular patch of the image (f) Ground truth image (g) segmented blood vessel.

This algorithm is tested on hospital images for calculating the accuracy. The accuracy of a test is its ability to differentiate the blood vessel and non blood vessel correctly. To estimate the accuracy of a test, we should calculate the proportion of true positive and true negative in all evaluated cases. Mathematically, this can be stated as:

$$\text{Accuracy} = \frac{TP + TN}{TP + TN + FP + FN}$$

TP-Blood vessel area FP-Non blood vessel area

The average accuracy for the classification of blood vessel is 95.64%.

II) Optic Cup And Disc Segmentation

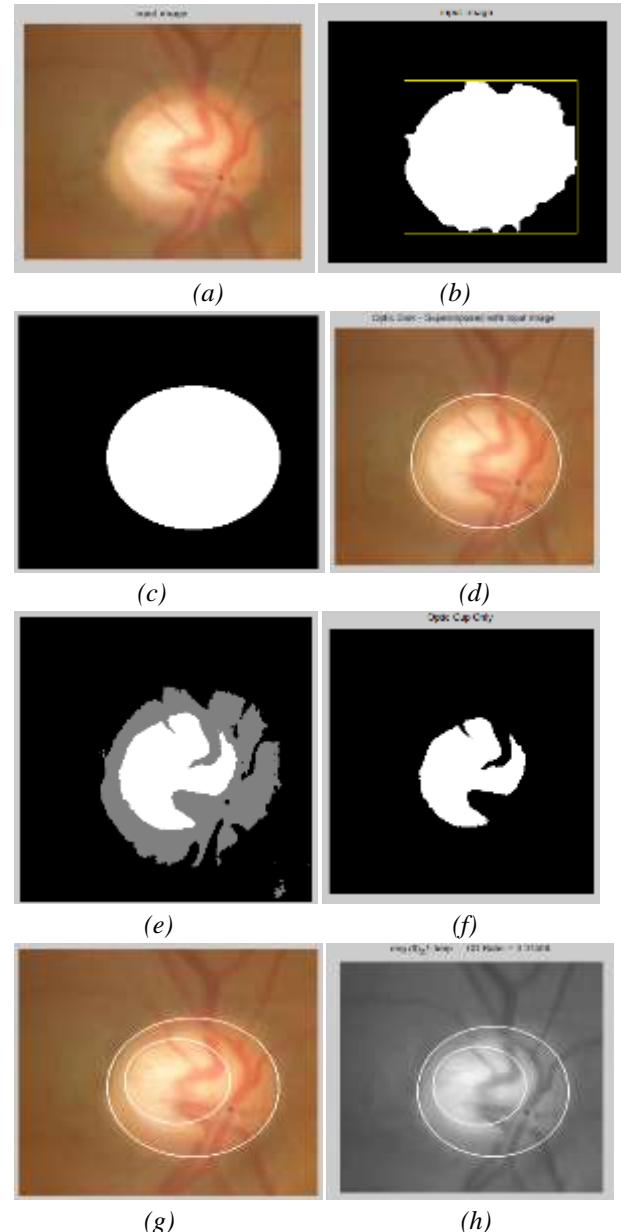


Fig.11: (a)ROI detection ,(b)Ground truth image,(c)Bounding ellipse,(d)Segmented optic disc,(e) Cup and disc (f) segmented cup(g) Ellipsefitting,(h) CDR calculation

TABULAR FORM II

IMAGE	CDR VALUE	CONDITION OF THE IMAGE
1	0.51	GLAUCOMA
2	0.37	HEALTHY
3	0.26	HEALTHY
4	0.51	GLAUCOMA
5	0.43	HEALTHY

V. DISCUSSION AND CONCLUSION

This study brings evidence that deep neural networks are a viable methodology for medical imaging, even though they solve the task in question in a different way than virtually all well-documented past work. We find this encouraging, in particular given the entirely supervised character of the neural approach, which learns from raw pixel data and does not rely on any prior domain knowledge on vessel structure. While learning, a network autonomously extracts low-level features that are invariant to small geometric variations, then gradually transforms and combines them into higher-order features. In this way, the raw raster image is transformed into a more abstract and a priori unknown representation that fosters effective vessel segmentation. The features learned at multiple levels of abstraction are then automatically composed into a complex function that maps an input patch to its label.

An average accuracy of 95.64% is determined in the classification of blood vessel or not. Optic cup is also segmented from the optic disc by Fuzzy C Means Clustering (FCM). This proposed algorithm is tested on a sample of hospital images and CDR value is determined. The obtained values of CDR is compared with the given values of the sample images and hence the performance of proposed system in which Convolutional Neural Networks for segmentation is employed, is excellent in automated detection of healthy and Glaucoma images.

REFERENCES

- [1] A. Hoover, V. Kouznetsova, and M. Goldbaum, "Locating blood vessels in retinal images by piecewise threshold probing of a matched filter response," *IEEE Transactions on Medical Imaging*, vol. 19, pp. 203–210, 2000.
- [2] R. Rangayyan, F. Oloumi, F. Oloumi, P. Eshghzadeh-Zanjani, and F. Ayres, "Detection of blood vessels in the retina using gabor filters," in *Canadian Conference on Electrical and Computer Engineering*, 2007, pp. 717–720.
- [3] A. Mendonca and A. Campilho, "Segmentation of retinal blood vessels by combining the detection of centerlines and morphological reconstruction," *IEEE Transactions on Medical Imaging*, vol. 25, no. 9, pp. 1200–1213, 2006.
- [4] M. Miri and A. Mahloojifar, "Retinal image analysis using curvelet transform and multistructure elements morphology by reconstruction," *IEEE Transactions on Biomedical Engineering*, vol. 58, no. 5, pp. 1183–1192, 2011.
- [5] K. A. Vermeer, F. M. Vos, H. G. Lemij, and A. M. Vossepoel, "A model based method for retinal blood vessel detection," *Computers in Biology and Medicine*, vol. 34, no. 3, pp. 209–219, 2004.
- [6] B. Lam and H. Yan, "A novel vessel segmentation algorithm for pathological retina images based on the divergence of vector fields," *IEEE Transactions on Medical Imaging*, vol. 27, no. 2, pp. 237–246, 2008.
- [7] Y. Bengio, P. Lamblin, D. Popovici, H. Larochelle et al., "Greedy layer-wise training of deep networks," *Advances in neural information processing systems*, vol. 19, p. 153, 2007.
- [8] M. Fraz, P. Remagnino, A. Hoppe, B. Uyyanonvara, A. Rudnicka, C. Owen, and S. Barman, "Blood vessel segmentation methodologies in retinal images - a survey," *Comput. Methods Prog. Biomed.*, vol. 108, no. 1, pp. 407–433, Oct. 2012. [Online].
- [9] J. Staal, M. D. Abramoff, M. Niemeijer, M. A. Viergever, and B. van Ginneken, "Ridge-based vessel segmentation in color images of the retina," *Medical Imaging, IEEE Transactions on*, vol. 23, no. 4, pp. 501–509, 2004.
- [10] A. Hoover, V. Kouznetsova, and M. Goldbaum, "Locating blood vessels in retinal images by piecewise threshold probing of a matched filter response," *Medical Imaging, IEEE Transactions on*, vol. 19, no. 3, pp. 203–210, 2000.
- [11] C. G. Owen, A. R. Rudnicka, R. Mullen, S. A. Barman, D. Monekso, P. H. Whincup, J. Ng, and C. Paterson, "Measuring retinal vessel tortuosity in 10-year-old children: validation of the computer-assisted image analysis of the retina (caiar) program," *Investigative ophthalmology & visual science*, vol. 50, no. 5, pp. 2004–2010, 2009.
- [12] E. Ricci and R. Perfetti, "Retinal blood vessel segmentation using line operators and support vector

- classification,” *Medical Imaging, IEEE Transactions on*, vol. 26, no. 10, pp. 1357–1365, 2007.
- [13] F. M. Villalobos-Castaldi, E. M. Felipe-Riverón, and L. P. Sánchez-Fernández, “A fast, efficient and automated method to extract vessels from fundus images,” *J. Vis.*, vol. 13, no. 3, pp. 263–270, Aug. 2010.
- [14] G. Azzopardi, N. Strisciuglio, M. Vento, and N. Petkov, “Trainable cosfire filters for vessel delineation with application to retinal images,” *Medical image analysis*, vol. 19, no. 1, pp. 46–57, 2015.
- [15] Y. Zhao, L. Rada, K. Chen, S. P. Harding, and Y. Zheng, “Automated vessel segmentation using infinite perimeter active contour model with hybrid region information with application to retinal images,” *Medical Imaging, IEEE Transactions on*, vol. 34, no. 9, pp. 1797–1807, 2015.
- [16] J. V. Soares, J. J. Leandro, R. M. Cesar Jr, H. F. Jelinek, and M. J. Cree, “Retinal vessel segmentation using the 2-d gabor wavelet and supervised classification,” *Medical Imaging, IEEE Transactions on*, vol. 25, no. 9, pp. 1214–1222, 2006.
- [17] S. Roychowdhury, D. D. Koozekanani, and K. K. Parhi, “Blood vessel segmentation of fundus images by major vessel extraction and subimage classification,” *Biomedical and Health Informatics, IEEE Journal of*, vol. 19, no. 3, pp. 1118–1128, 2015.
- [18] X. You, Q. Peng, Y. Yuan, Y. Cheung, and J. Lei, “Segmentation of retinal blood vessels using the radial projection and semi-supervised approach,” *Pattern Recogn.*, vol. 44, pp. 2314–2324, 2011.
- [19] World health organization programme for the prevention of blindness and deafness- global initiative for the elimination of avoidable blindness World health organization, Geneva, Switzerland, WHO/PBL/97.61 Rev.1, 1997.
- [20] G. Michelson, S. Wrtges, J. Hornegger, and B. Lausen, “The papilla as screening parameter for early diagnosis of glaucoma,” *Deutsches Aerteblatt Int.*, vol. 105, pp. 34–35, 2008.
- [21] P. L. Rosin, D. Marshall, and J. E. Morgan, “Multimodal retinal imaging: New strategies for the detection of glaucoma,” in *Proc. ICIP*, 2002.
- [22] M.-L. Huang, H.-Y. Chen, and J.-J. Huang, “Glaucoma detection using adaptive neuro-fuzzy inference system,” *Expert Syst. Appl.*, vol. 32, no. 2, pp. 458–468, 2007.
- [23] G. D. Joshi, J. Sivaswamy, K. Karan, and S. Krishnadas, “Optic disk and cup boundary detection using regional information,” in *Biomedical Imaging: From Nano to Macro, 2010 IEEE International Symposium on*, 2010, pp. 948–951.
- [24] U. R. Acharya, S. Dua, X. Du, S. Vinitha Sree, and C. K. Chua, “Automated diagnosis of glaucoma using texture and higher order spectra features,” *Information Technology in Biomedicine, IEEE Transactions on*, vol. 15, pp. 449–455, 2011.
- [25] C. Burana-Anusorn, W. Kongprawechnon, T. Kondo, S. Sintuwong, and K. Tungpimolrut, “Image Processing Techniques for Glaucoma Detection Using the Cup-to-Disc Ratio,” *Thammasat International Journal of Science and Technology*, vol. 18, p. 22, 2013.
- [26] G. D. Joshi, J. Sivaswamy, and S. Krishnadas, “Optic disk and cup segmentation from monocular color retinal images for glaucoma assessment,” *Medical Imaging, IEEE Transactions on*, vol. 30, pp. 1192–1205, 2011.
- [27] S. Chandrika and K. Nirmala, “Analysis of CDR Detection for Glaucoma Diagnosis,” *International Journal of engineering research and application (IJERA) ISSN*, pp. 2248–9622.
- [28] C. Burana-Anusorn, W. Kongprawechnon, T. Kondo, S. Sintuwong and K. Tungpimolrut, *Image processing techniques for glaucoma detection using the cup-to-disc ratio*, in *Thammasat International Journal of Science and Technology*, January Mar 2013, vol. 19, No. 1, pp. 22–34.
- [29] Hrynchak P., Hutchings N, Jones D. and Simpson T., *A comparison of cup-to-disc ratio measurement in normal subjects using optical coherence tomography image analysis of the optic nerve head and stereo fundusbiomicroscopy.*, in *Touch Briefings 2012*. pp. 92–97.
- [30] A. SC Reis, A. Toren and M. T. Nicolela, *Clinical optic disc evaluation in glaucoma.*, in *Ophthalmic Physiol Opt.* vol.6 Nov 24, 2004 pp. 543–550